Proc. Natl. Acad. Sci. USA
Vol. 91, pp. 7797–7801, August 1994
Neurobiology

Formation of receptive fields in realistic visual environments according to the Bienenstock, Cooper, and Munro (BCM) theory

(synaptic modification/visual cortex/natural images)

C. CHARLES LAW AND LEON N COOPER*

Department of Physics and Neuroscience, Institute for Brain and Neural Systems, Brown University, Box 1843, Providence, RI 02912

Contributed by Leon N Cooper, April 4, 1994

ABSTRACT **The Bienenstock, Cooper, and Munro (BCM) theory of synaptic plasticity has successfully reproduced the development of orientation selectivity and ocular dominance in kitten visual cortex in normal, as well as deprived, visual environments. To better compare the consequences of this theory with experiment, previous abstractions of the visual environment are replaced in this work by real visual images with retinal processing. The visual environment is represented by 24 gray-scale natural images that are shifted across retinal fields. In this environment, the BCM neuron develops receptive fields similar to the fields of simple cells found in kitten striate cortex. These fields display adjacent excitatory and inhibitory bands when tested with spot stimuli, orientation selectivity when tested with bar stimuli, and spatial-frequency selectivity when tested with sinusoidal gratings. In addition, their development in various deprived visual environments agrees with experimental results.**

In 1982 Bienenstock, Cooper, and Munro (BCM) proposed a concrete synaptic-modification hypothesis in which two regions of modification (Hebbian and anti-Hebbian) are stabilized by the addition of a sliding modification threshold (1). The theory was created originally to explain the development of orientation selectivity of visual cortical neurons in various visual environments. This theory has since proven capable of also explaining ocular dominance and selective response properties in the most diverse visual environments, one of the most thoroughly studied areas in neuroscience. In this paper we examine the consequences of the replacement of previous abstractions of the visual environment by real visual images with retinal processing.

During a critical period of postnatal development, the response properties of neurons in striate cortex of the kitten can be modified by manipulating the visual experience of the animal (2–4). Clothiaux, Bear, and Cooper (CBC) (5) showed that simulations based on the BCM theory, with a fixed set of parameters, reproduce both the kinetics and equilibrium states of experience-dependent modifications that are observed experimentally in these neurons. The rearing conditions that they simulated include normal rearing, monocular deprivation, reverse suture, strabismus, and binocular deprivation.

An important simplification used in all previous BCM simulations is the assumed activity of neurons in the lateral geniculate nucleus (LGN) resulting from visual experience. In CBC, for example, an abstract set of 12 patterns represents the activity on geniculo–cortical afferents supposedly resulting from contoured stimuli with 12 different orientations. LGN activity in a normal visual environment is modeled as this patterned input distorted by noise. In the absence of visual contours, LGN–cortical input activity is assumed to be uncorrelated noise distributed around spontaneous activity. The justification for this simplification is that the visual fields of neurons in primary visual cortex are small, so that reproducible visual contours when viewed through this aperture are most likely to be noise-like or edges distorted by noise, allowing visual input to be represented by a pattern set with a single variable representing the orientation of the stimulus.

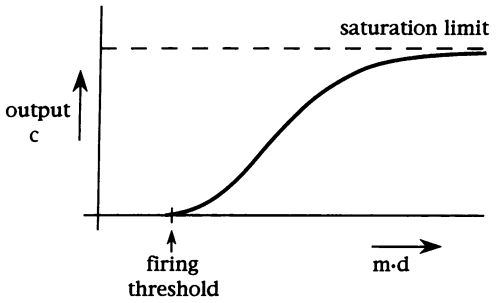

FIG. 1. Sigmoidal activation function. m, Strength of the synapses that connect the input d to the BCM neuron and the sigmoidal function σ.

In this paper we replace this simplification by a more realistic visual environment. By so doing we can investigate the behavior of BCM neurons subjected to input from LGN more like that actually experienced in normal and deprived situations. In addition, we can examine the validity of previous assumptions.

METHODS

Modification of synaptic weights in the BCM theory is given by

$$\dot{m}_i = \eta\phi(c, \Theta)d_i, \qquad [1]$$

where cell activity measured relative to spontaneous activity is

$$c = \sigma(\mathbf{m}\cdot\mathbf{d}). \qquad [2]$$

The vector $\mathbf{m}$ represents the strength of the synapses that connect the input $\mathbf{d}$ to the BCM neuron and the sigmoidal function σ (Fig. 1). The constant η determines the learning speed, and the function ϕ is

$$\phi(c, \Theta) = (\Theta^{-1})c(c - \Theta). \qquad [3]$$

This equation differs from that used in ref. 6 by the factor Θ^{-1}, which does not affect the position or the stability of fixed points but does affect the rate at which these fixed points are reached. Because Θ changes very slowly, the term acts as a

The publication costs of this article were defrayed in part by page charge payment. This article must therefore be hereby marked "*advertisement*" in accordance with 18 U.S.C. §1734 solely to indicate this fact.

Abbreviations: BCM, Bienenstock, Cooper, and Munro; CBC, Clothiaux, Bear, and Cooper; LGN, lateral geniculate nucleus.

*To whom reprint requests should be addressed.

Table 1. Parameters of the model

Parameter	Significance	Value
R_r, units	Radius of the retinal patches	5.0
STD_c, units	SD of a ganglion excitatory-center Gaussian distribution	1.0
STD_s, units	SD of a ganglion inhibitory-surround Gaussian distribution	3.0
d_s, Hz	Level of ganglion spontaneous activity	20.0
c_s, Hz	Level of cortical-neuron spontaneous activity	1.0
$\overline{n^2}$, Hz^2	Average square of the ganglion noise from a sutured eye	3.0
$m_j(0)$	Starting value of the synaptic weights for normal rearing	0.0–0.001
η	Modification step size	0.000001
τ, iterations	Time constant in the definition of Θ	1000

variable learning rate, speeding up the simulation when the neuron is far from a fixed point (Θ small) and slowing the simulation when Θ and the weights grow large. Thus, the simulations are more stable and less dependent on initial conditions.† Following ref. 6 the sliding threshold Θ is defined as the second moment of the cell activity.

$$\Theta = (\tau^{-1} \int_{-\infty}^{t} dt' c^2 e^{\tau^{-1}(t'-t)}), \quad [4]$$

where the time constant τ determines how rapidly the threshold moves. The parameter set used for the simulations described here are given in Table 1.

†We note the obvious: Only some qualitative features of ϕ (such as the negative and positive regions, the zero crossings, and the moving threshold) are required to explain present experimental data. The detailed form of this function will be determined by further sophisticated experiment, analysis, and simulation.

REALISTIC VISUAL ENVIRONMENT

An added feature of the simulations described below is the method by which the visual environment is represented. Real two-dimensional natural images processed using simple retinal models are used as visual inputs. Circular regions from the left and the right retinas are used to generate activity in the thalamocortical projections. The LGN is assumed to simply relay the signal generated by the retina to the visual cortex.

To model the visual environment, we use 24 gray-scale images with dimensions of 256 × 256 pixels. The retinas are composed of square arrays of receptors and ganglion cells spaced one unit apart. Each ganglion cell has an antagonistic center–surround receptive field that approximates a difference of two Gaussian distributions. The SD of the surround Gaussian distribution is three times larger than the SD of the center Gaussian distribution. The resulting receptive field center has a radius of 2.22 units. The ganglion-cell receptive

FIG. 2. Some of the 24 natural images used to represent the visual environment. The receptive field circle determines the current input and moves randomly over the images.

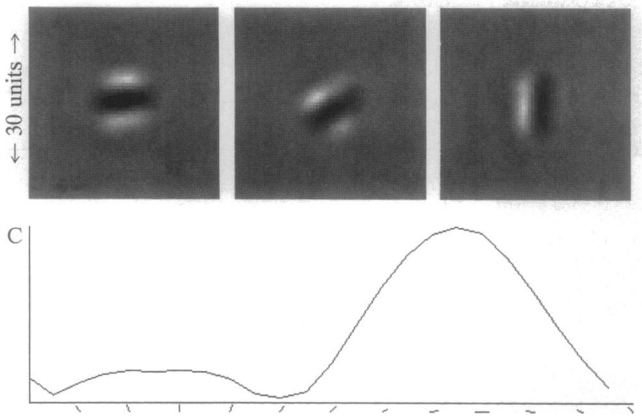

FIG. 3. (*Upper*) Receptive fields developed by a BCM neuron in a realistic visual environment. The neuron had input from a patch of the retina with a diameter of 10.0 units. The light areas of the receptive field map represent excitatory regions, and the dark areas represent inhibitory regions. (*Lower*) Orientation tuning curve generated with bars of light as described in the text. C, output.

fields are balanced so that uniform illumination of any intensity results in spontaneous activity. Cell activity is measured relative to spontaneous activity, and the nonlinearity in σ restricts the *absolute* ganglion-cell activity to be positive.

For each cycle of the simulation, the activity of the receptors in the retina is determined by randomly picking one of the 24 images and randomly shifting the receptive field circle (Fig. 2). The shift is restricted so that none of the ganglion-cell receptive field centers fall within 10 units of the image border. The activity of each receptor in the model is determined by the intensity of a pixel in the image. Obviously, this generates a very large training set and, in contrast to what was done previously, we need make no assumptions concerning relative frequency of patterns and noise.

METHOD OF TESTING THE RECEPTIVE FIELD OF THE BCM NEURON

At selected times during the simulations, the properties of the BCM neurons are tested separately through the left and right eyes. Two-dimensional maps of the receptive field are generated by "shining" small (radius = 0.8 unit) spots of light on the retina at many locations and recording the cortical neuronal activity generated for each spot. This technique is similar to the process used by Jones and Palmer (7) to generate two-dimensional receptive-field profiles of simple cells in cat striate cortex. For simplicity, low-contrast spots are used to avoid both the ganglion-cell and the BCM-neuron nonlinearities. Orientation tuning of the neuron is determined by presenting bars of light. For each orientation several bar stimuli (width = 2 units) are generated at different spatial locations. The best response to the set of stimuli determines the amplitude of the tuning curve for that orientation. The maxima of the left- and right-eye tuning curves are then used to determine the binocularity of the BCM neuron. Spatial-frequency selectivity is tested by using sinusoidal gratings at the best orientation of the neurons. For each frequency, many stimuli with various spatial phases are used to determine the maximal response of the neurons.

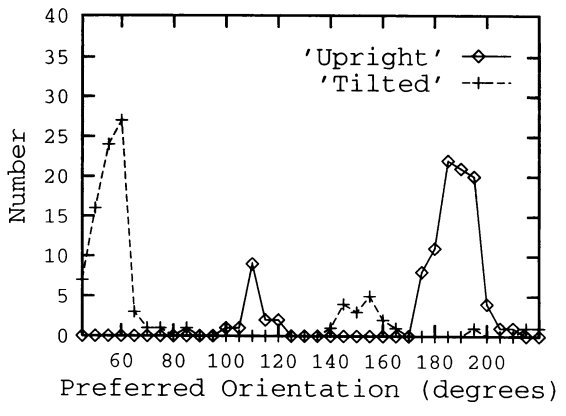

FIG. 4. Orientation preferences developed by 100 individual simulations of normal rearing trained with natural images and 100 simulations trained with natural images rotated by 45°.

RESULTS

Most important is the fact that replacement of previously employed simplifications by a realistic visual environment does not significantly alter simulation results. As in the simulations of CBC, normal rearing produces a selective binocular neuron that is equally responsive to stimulation through the left and right eyes; in binocular deprivation, the BCM neuron becomes less responsive and less selective but remains binocular; in monocular deprivation, the sutured eye disconnects from the BCM neuron, whereas in reverse suture the newly closed eye disconnects from the BCM neuron before the newly opened eye reconnects. Fig. 8 shows the results of the reverse suture simulation with natural images. These results, which will be described in more detail elsewhere, suggest that the 12 abstract patterns of CBC were adequate representations of visual experience for these deprivation simulations.

In simulations of normal rearing both eyes receive the same pattern input from the natural images. At the beginning of the simulation synaptic weights are initialized to small random values. Even though at this stage the cortical neuron is relatively unresponsive to visual stimuli, the initialization of the weights adds a small bias that can influence the final selectivity of the neuron. Fig. 3 shows the results of a single simulation that is initialized with random weights. At the end of normal rearing, the BCM neuron is binocular and has properties similar to simple cells found in striate cortex. Its receptive field has adjacent excitatory and inhibitory bands that produce selectivity to the orientation of bar stimuli. In our simulations, the BCM neuron most often becomes selective to horizontal and vertical orientations. The preference for horizontal and vertical stimuli is a property of the natural images and is not a

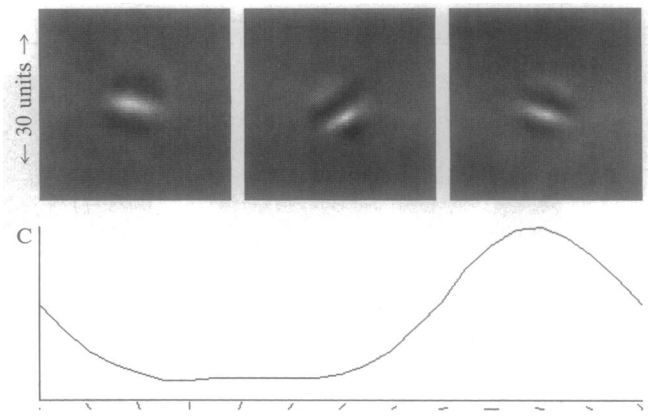

FIG. 5. Receptive field (*Upper*) and orientation selectivity (*Lower*) developed in the natural visual environment without retinal preprocessing. Addition of retinal preprocessing makes little difference to the selectivity developed by the BCM neuron. C, output.

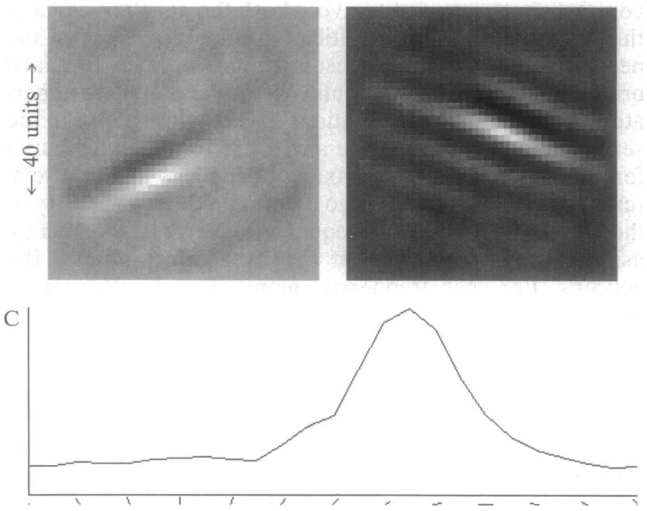

FIG. 6. Receptive fields (*Upper*) and typical selectivity (*Lower*) generated by the cortical neuron. The size of the retinal patches that connect to the BCM neuron is four times larger than previous simulations. Except for an elongated receptive field, the properties of the BCM neuron are similar to simulations with input that has a smaller spatial extent. C, output.

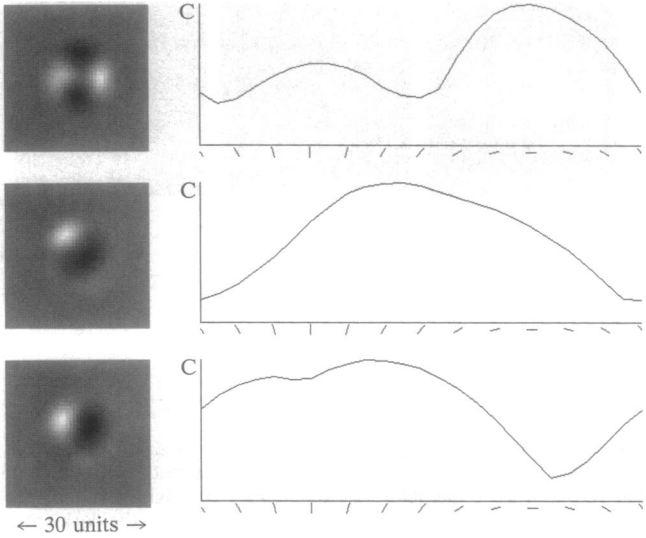

FIG. 7. Receptive fields (*Left*) and orientation selectivity (*Right*) for three single-cell simulations in an environment of correlated noise. The only difference between the simulations is the initialization of synaptic weights. C, output.

spurious bias introduced by the retinal or cortical models. When the environment is rotated by rotating the natural images, the orientation preference of the model also shifts. Fig. 4 shows orientation-preference histograms generated in two ways: the first uses the normal visual environment, whereas the second uses a visual environment rotated by 45°. Each histogram represents data from 100 simulations.

The results of these simulations are very robust. Changing the parameters of the retina does not significantly alter the simulations. Even completely bypassing the retina has little effect on the selectivity developed. However, it does change the rate at which the fixed points are reached. Fig. 5 shows the receptive field developed when the BCM neuron is trained directly from the natural images.

The receptive fields developed by the BCM neuron also are not significantly dependent on the size of the retinal patches that project to the cortical neuron. When simulations are run with much larger retinas, the BCM neuron simply disconnects from most of the ganglion cells. Fig. 6 shows the receptive field when the retinal diameter is four times larger than the diameter of the retina in the simulation displayed in Fig. 3.

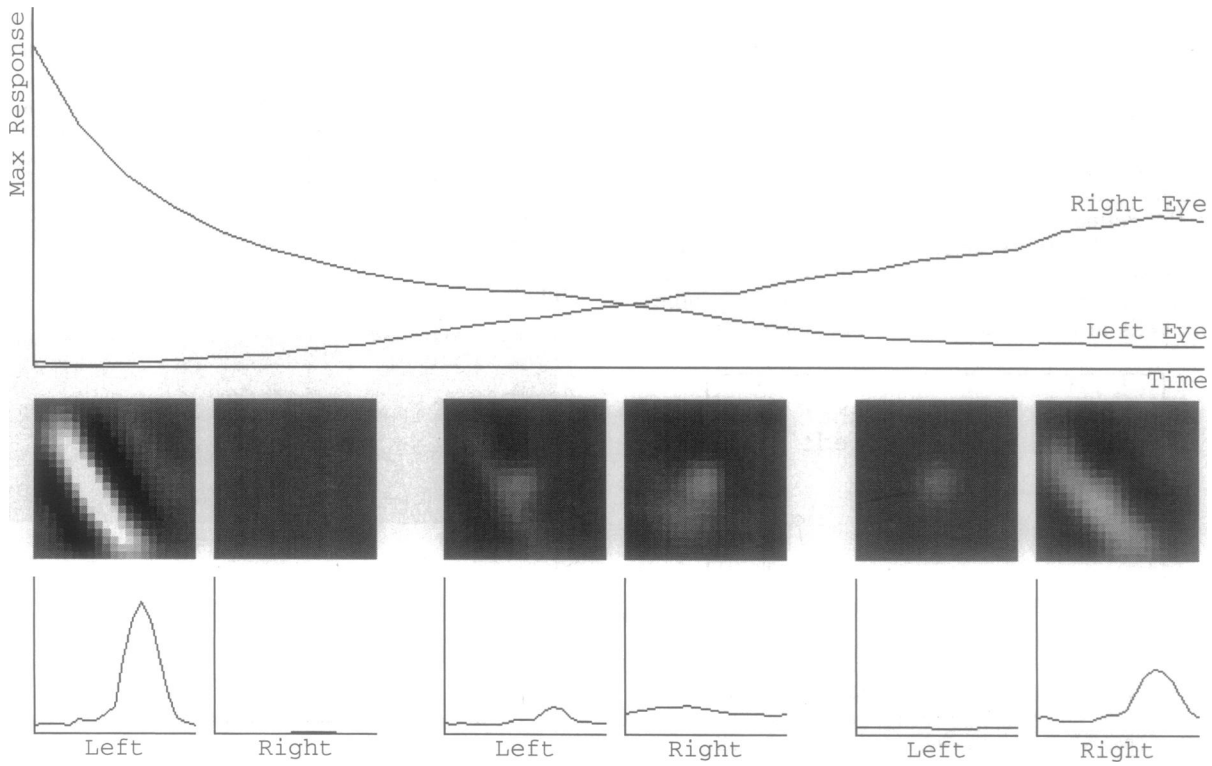

FIG. 8. Reverse suture simulation results. (*Top*) The graph displays the maximum (Max) responsiveness of the BCM neuron to stimulation through the left and right eyes. (*Middle*) The receptive field of the cortical neuron at three different times during the simulation, tested through the left and right eyes separately. (*Bottom*) Orientation tuning as tested through the left and right eyes separately.

Mastronarde (8) observed that the activities of neighboring ganglion cells are correlated in the absence of contour vision, and it has been suggested (9) that such activity could play an important role in the formation of receptive fields before any contoured visual experience.

Although the BCM modification algorithm usually is applied to account for cortical neuron response in normal and deprived visual environments, we have simulated the development of BCM neurons in an environment of correlated noise to model spontaneous activity that might occur before visual experience. Small-amplitude, uncorrelated noise is presented as visual input, and the antagonistic center–surround receptive fields in the retina produce positive correlations at small distances (<2.2 units) and negative correlations at medium distances (>2.2 units).

In this environment the BCM neuron develops receptive fields with distinct excitatory and inhibitory regions (Fig. 7). However, the neurons trained with such correlated noise do not become as selective to features such as orientation and spatial frequency as neurons trained with natural images. These results are consistent with the idea that although some selectivity may develop in primary visual cortex before visual experience, maturation to adult levels of selectivity requires contoured visual experience.

DISCUSSION

The development of BCM neurons in realistic visual environments is very similar to that presented previously with various simplifications. Normal rearing produces selective binocular neurons equally responsive to stimulation through left and right eyes. For the various deprived environments we obtain results qualitatively similar to these reported by CBC. What differences occur may actually bring us in closer agreement with observations. For example, in simulations of reverse suture the realistic visual environment eliminates a possible discrepancy between experimental findings and the CBC simulations. It was noted by Mioche and Singer (10) that the recovery of the newly opened eye is slow and incomplete after reverse suture; in the CBC simulation the neuron has a fast and robust recovery. As suggested in CBC (5), this has several possible explanations. However, the present simulation of reverse suture displayed in Fig. 8, without any additional assumptions, agrees more closely with the experimental findings: the BCM neuron does recover responsiveness to the newly opened eye, but recovery is slow.

We have also shown that the BCM theory is consistent with the hypothesis that correlated retinal spontaneous activity could be responsible for the development of some selectivity before visual experience. Crude orientation selectivity forms in the absence of contoured visual experience when the visual environment after retinal preprocessing is correlated noise. These results are consistent with the view that although some selectivity may develop in the absence of contoured vision, normal visual experience is necessary to develop full selectivity.

We thank the members of the Institute for Brain and Neural Systems for many conversations and, in particular, Ms. Tomoko Ozeki for her assistance in running some of the simulations. This work was supported, in part, by the Office of Naval Research, the Army Research Office, and the National Science Foundation.

1. Bienenstock, E. L., Cooper, L. N & Munro, P. W. (1982) *J. Neurosci.* **2**, 32–48.
2. Buissert, P. & Imbert, M. (1976) *J. Physiol. (London)* **255**, 511–525.
3. Hubel, D. H. & Wiesel, T. N. (1970) *J. Physiol. (London)* **206**, 419–436.
4. Wiesel, T. N. & Hubel, D. H. (1963) *J. Neurophysiol.* **26**, 1003–1017.
5. Clothiaux, E. E., Bear, M. F. & Cooper, L. N (1991) *J. Neurophysiol.* **66**, 1785–1805.
6. Intrator, N. & Cooper, L. N (1992) *Neural Networks* **5**, 3–17.
7. Jones, J. P. & Palmer, L. A. (1987) *J. Neurophysiol.* **58**, 1187–1258.
8. Mastronarde, D. N. (1989) *Trends Neurosci.* **12**, 75–80.
9. Miller, K. D., Keller, J. B. & Stryker, M. P. (1989) *Science* **245**, 605–615.
10. Mioche, L. & Singer, W. (1989) *J. Neurophysiol.* **62**, 185–197.